J. Chem. Soc., Faraday Trans. 2, 1983, 79, 719–730

Molecular Dynamics of Liquid and Supercooled Ethyl Chloride

A Computer Simulation

BY MYRON W. EVANS

Chemistry Department, University College of Wales, Aberystwyth SY23 1NE

Received 7th October, 1982

The computer simulation method has been used to investigate the molecular dynamics of liquid ethyl chloride at 293 K, under its own vapour pressure, and supercooled at 118 K. The molecular diffusion at both state points is anisotropic, involving strong rotation/translation coupling. In the supercooled condition the orientational autocorrelation function of the dipole unit vector decays almost infinitely slowly, implying the existence of a dielectric loss at very low frequencies (α, or α, β type). The (α, β, γ) theory of dielectric loss, formulated by Evans and Reid, is corroborated by this first computer simulation of the γ process, which appears in the far-infrared.

The ethyl chloride molecule is an example of a low-symmetry asymmetric top (C_1 or lower) whose dipole moment does not lie in an axis of the principal moment of inertia frame (fig. 1). The liquid boils under 1 bar at 285 K. For either or both of these reasons it has not been investigated in any depth as regards the nature of its molecular dynamics. There seems to be only one (n.m.r.) paper in the whole of the literature on the relaxational properties of ethyl chloride molecules in the liquid state.[1] This contrasts remarkably with the two hundred or more papers available on a C_{3v} chlorinated methane such as chloroform, whose dynamical properties are less interesting because of the relatively higher symmetry.

In this paper we aim to demonstrate the ability of the molecular dynamics computer simulation method to probe the nature of low-symmetry asymmetric-top molecular dynamics. The ethyl chloride potential is constructed on a site–site basis from the successful 5×5 site–site model of Lassier and Brot[2] for t-butyl chloride. The ethyl chloride potential is obtained simply by replacing two methyl Lennard-Jones/point-charge sites by two hydrogens. This reduces the symmetry from C_{3v} to C_1 (or less) and completely changes the molecular-dynamical characteristics. In order to maintain a consistent scheme of approach to the parametrisation of the pair potential we use the same CH_3, C and Cl atom–atom Lennard-Jones parameters as in an earlier simulation[3] of t-butyl chloride (in the liquid and rotator phases). The H parameters used are the same as those in earlier simulations[4] of CH_2Cl_2, $CHCl_3$, acetone, $CHBr_3$, CH_3I, CH_3CN and CH_3OH. For these C_{2v} or C_{3v} symmetric tops, well over a thousand papers are available on the molecular dynamics and interactions from a variety of spectroscopic sources. This information has been utilised[4] to test the effectiveness of the computer simulation, keeping to the same Lennard-Jones parameters for atom–atom interactions, and using literature values for point charges localised at the atomic sites to simulate the electrodynamics. The simulations are successful in many respects for the non-associated species (including acetone), but less so with CH_3I, CH_3CN and CH_3OH, for which polarisability, association and hydrogen-bonding effects are known to be important.

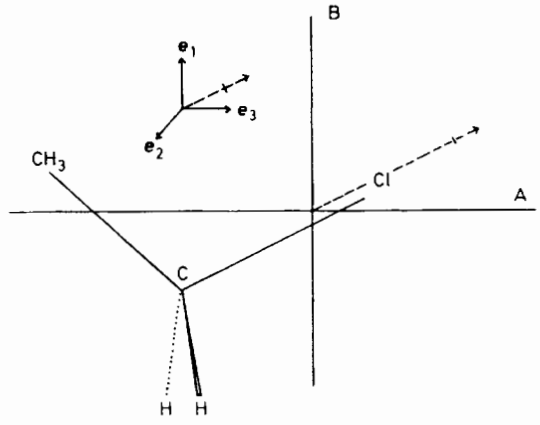

Fig. 1. Frame of reference for ethyl chloride. *A* and *B* are two of the three mutually perpendicular axes of the principal moments of inertia. These intersect at the centre of mass, which is close to the Cl site. *Inset*: The unit vectors e_1, e_2 and e_3 of the moment-of-inertia frame in relation to the dipole axis [dashed line in the direction of the C—Cl bond in the plane (e_1, e_3)].

The second virial coefficient of gaseous ethyl chloride is known with some accuracy[5–7] and does not indicate the presence of significant association or dimerisation. As in t-butyl chloride, therefore, the molecular interactions are probably dominated by Lennard-Jones type repulsion and dispersion and not by strong electrodynamic and polarisability effects, which are much more difficult to account for in a computer simulation. In marked contrast to t-butyl chloride, which has two well defined rotator phases,[2] ethyl chloride can be vitrified and the liquid supercooled.[8] On heating the glassy C_2H_5Cl, an endothermic process begins at a temperature T_V where the glass softens. It is transformed into a supercooled liquid by the appearance of free volume (holes). At a temperature T_R the supercooled liquid recrystallises. X-ray powder spectra indicate that there is no crystallisation below T_R. Infrared spectra prove that in the glassy and supercooled liquid states of the alkyl chlorides the same rotational isomers coexist that are observed in the liquid above the melting point. In the general case of n-alkyl halide crystals, only the *trans* isomer exists. N.m.r. spectra show that between T_V and T_R a dynamic reorientation of the different segments of the hydrocarbon chain appears, which ceases in the crystal. The existence of an intense dielectric absorption between T_V and T_R confirms the reorientation of the polar group CH_2X, which is related[8] to the appearance of 'holes' in the liquid. For ethyl chloride the reorientation of $-CH_2Cl$ implies, in our model, the reorientation of the whole molecule.

The total electric polarisation of C_2H_5Cl has been measured in the gaseous state by Barnes *et al.*[9] at various temperatures, and the density and complex permittivity over the liquid range by McMullen *et al.*[10] The density ranges from 0.9214 gm cm^{-3} at 273 K to 1.1281 g cm^{-3} in the supercooled liquid at 118.3 K. In the solid at 112.9 K the density increases to 1.139 gm cm^{-3}. The dielectric loss above 203 K is small up to 8 MHz, but the loss process begins to appear at the highest frequencies below this temperature and increases with decreasing temperature until the freezing point. The dipole moment is 2.00 D from the Onsager equation at 254.3 K and 1.90 D at 135.5 K. There is enough basic information available in the literature, therefore, to attempt a computer simulation of ethyl

chloride in the liquid and supercooled conditions. The effectiveness of the simulation can be measured by, for example, far-infrared measurements[11] on these phases.

Neutron scattering spectroscopy has been used[12] to observe the C—C—Cl deformation and Me torsional modes of ethyl chloride in the liquid and solid states and the torsional frequency of the methyl-group internal rotation assigned[13] at 278 cm^{-1}, which is clear of the far-infrared Poley absorption measured and reported here for the first time using computer simulation.

COMPUTER SIMULATION METHOD

The algorithm is based on a SERC CCP5 listing modified as described elsewhere.[3,4] The potential between two ethyl chloride molecules is simulated with a 5×5 site–site model consisting of atom–atom Lennard-Jones interactions plus partial charges localised on the atom sites. These were obtained from a paper by Mark *et al.*,[14] who calculated a dipole of 1.86 D from values[15] of $q_{CH_3} = 0.0465$, $q_C = -0.0502$, $q_H = 0.0808$ and $q_{Cl} = -0.157$, in units of $|e|$. The site–site Lennard-Jones parameters are as follows:[2–4] ε/k(Cl—Cl) = 127.9 K, σ(Cl—Cl) = 3.6 Å, ε/k(C—C) = 35.8 K, σ(C—C) = 3.4 Å, $\varepsilon/k(CH_3—CH_3)$ = 158.6 K, $\sigma(CH_3—CH_3)$ = 4.0 Å, ε/k(H—H) = 10.0 K and σ(H—H) = 2.8 Å.

The equations of rotational and translational motion are then solved with the same basic predictor–corrector routine following the standard methods of computer simulation. The 108 ethyl chloride molecules are initially arranged on a face-centred cubic lattice, which melts to a liquid over *ca.* 2000 time-steps of 5×10^{-15} s each. By suddenly dropping the temperature a simulation can also be effected of the supercooled and vitreous states. The room-temperature liquid was simulated at 293 K, $d = 0.8978$ gm cm^{-3} and the supercooled liquid at 118 K, $d = 1.1281$ gm cm^{-3}. The liquid boils at 285 K, 1 bar, so that the simulated liquid state at 293 K is that under slightly more than an atmosphere of its vapour pressure.

After a 2000 time-step run at equilibrium, the data are stored on disk and autocorrelation functions constructed by running-time averaging. Autocorrelation functions can be constructed of orientation vectors, $\boldsymbol{e}_1$, $\boldsymbol{e}_2$ and $\boldsymbol{e}_3$, fixed in the moment-of-inertia frame of the molecule, for angular variables such as the angular momentum ($\boldsymbol{J}$) and angular velocity ($\boldsymbol{\omega}$) and linear variables such as the centre-of-mass velocity ($\boldsymbol{v}$). By transforming the angular momentum ($\boldsymbol{J}$) and linear velocity ($\boldsymbol{v}$) into a rotating frame of reference, defined as the principal moment-of-inertia frame, and constructing the elements of $\langle \boldsymbol{v}(t)\boldsymbol{J}^T(0) \rangle$ in this frame, the details of rototranslational motion in ethyl chloride can be investigated directly. All the six off-diagonal elements of this matrix exist in principle for ethyl chloride because of the low, C_1, symmetry.

RESULTS AND DISCUSSION

THERMODYNAMICS

Some thermodynamical parameters are available from the computer simulation. These should be assessed in the spirit of this work, which is not intended as an exercise in obtaining an accurate pair potential, but rather as an effort to outline a range of dynamic properties in a self-consistent manner.

At 293 K (input), the total energy is -18.06 kJ mol^{-1}, the translational temperature (after *ca.* 1000 steps into equlibrium) is 292 K, the rotational temperature is 299 K, translational kinetic energy is 36.4 kJ mol^{-1}, the rotational kinetic energy is 37.3 kJ mol^{-1} and the total energy is negative and constant to within $\pm 0.1\%$.

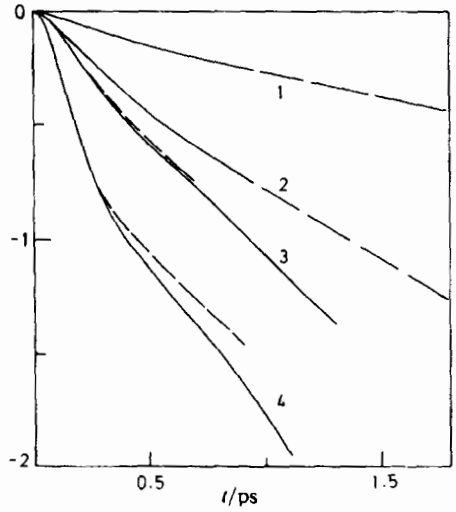

Fig. 2. Orientational autocorrelation functions at 293 K; first (P_1) and second (P_2) rank Legendre polynomials. (1) $P_1(e_3)$, (2) $P_2(e_3)$, (3) $P_1(e_1)$, (4) $P_2(e_1)$, (– – –, 3) $P_1(e_2)$ and (– – –, 4) $P_2(e_2)$.

At 118 K (input) the values are: -27.8 kJ mol^{-1}, 117.7 K, 117.8 K, 14.7 kJ mol^{-1}, 14.7 kJ mol^{-1} and $\pm 0.1\%$ respectively.

DYNAMICS

The only available literature relaxation time for liquid ethyl chloride is the n.m.r. spin–spin time of Miller and Gordon.[1] This is derived from modelling techniques assuming that the rotational diffusion is isotropic. It must therefore be regarded as a first approximation. It is not clear at what temperature these authors carried out their work, the quoted range being 301–308 K. The derived second-rank orientational correlation time[2] is 0.7 ± 0.1 ps. It is not clear to which vector this refers. The only other piece of relevant experimental evidence we have been able to find comes from the dielectric relaxation data of McMullen *et al.*[10] These data cover a wide temperature range, but do not extend to high enough frequencies to isolate at any temperature the peak of the Debye dielectric loss. The 293 K data imply that the loss peak corresponds to a relaxation time in the picosecond range.

COMPUTER SIMULATION – CORRELATION TIMES AND FUNCTIONS

LIQUID UNDER ITS OWN VAPOUR PRESSURE AT 293 K

The first (P_1) and second (P_2) rank orientational autocorrelation functions (a.c.f.) of the three unit vectors e_1, e_2 and e_3 are illustrated in fig. 2. These unit vectors are in the three axes of the principal moment-of-inertia frame illustrated in fig. 1. Wagner and Dailey[16] have measured the three principal moments of inertia of ethyl chloride by microwave spectroscopy and find it to be (fortuitously) almost an inertial symmetric top. The A axis of the principal moment-of-inertia frame subtends an angle of 26° 30′ with the direction of the C—Cl bond (fig. 1), which is approximately the direction of the resultant molecular dipole moment, μ. Band-shapes[11] of liquid ethyl chloride in the infrared, far-infrared and dielectric frequency

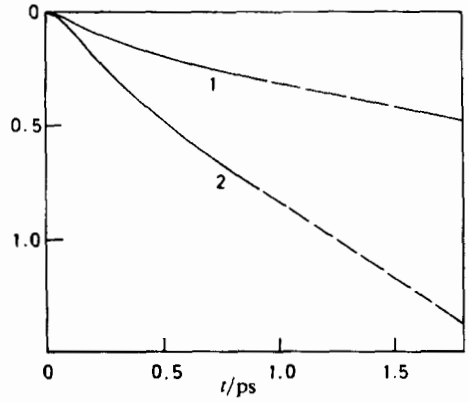

Fig. 3. As for fig. (2); (1) $P_1(\boldsymbol{u})$ and (2) $P_2(\boldsymbol{u})$, where $\boldsymbol{u}$ is the dipole unit vector.

regions depend on first-rank correlation functions of $\boldsymbol{\mu}$, and Raman and Rayleigh bandshapes on second-rank orientational correlation functions involving the molecular polarisability tensor $\boldsymbol{\alpha}$, which has a component in the direction of $\boldsymbol{\mu}$. The frame of $\boldsymbol{\alpha}$ (or of $\boldsymbol{\mu}$) is not the same as that of the principal moments of inertia. There is, however, a simple relation between the unit vector $\boldsymbol{u} = \boldsymbol{\mu}/|\boldsymbol{\mu}|$ (the dipole unit vector) and $\boldsymbol{e}_1$ and $\boldsymbol{e}_3$. This takes the form (fig. 1):

$$\boldsymbol{u} = x\boldsymbol{e}_1 + y\boldsymbol{e}_3 \tag{1}$$

where x and y are numbers, if we assume that $\boldsymbol{u}$ lies in the C—Cl bond, which is correct to a good approximation.

Eqn (1) allows us to compute the first- and second-rank orientational a.c.f. of $\boldsymbol{u}$, illustrated in fig. 3. Neglecting cross-correlations and internal field corrections, the Fourier transform of $P_1(\boldsymbol{\mu})$ is a measure of the dielectric loss spectrum, that of $\langle\dot{\boldsymbol{\mu}}(t)\cdot\dot{\boldsymbol{\mu}}(0)\rangle/\langle\dot{\boldsymbol{\mu}}(0)\cdot\dot{\boldsymbol{\mu}}(0)\rangle$ is the far-infrared spectrum. $P_2(\boldsymbol{\mu})$ can be obtained from the Raman spectrum of liquid ethyl chloride, or alternatively from the depolarised Rayleigh spectrum. Nuclear magnetic resonance relaxation of various types[1,3,4] can be used to measure the anisotropy of rotational diffusion in liquid ethyl chloride using reference vectors such as $\boldsymbol{e}_1$, $\boldsymbol{e}_2$ and $\boldsymbol{e}_3$. Fig. 2 shows that the anisotropy of the rotational diffusion in the moment-of-inertia frame is very large, two moments of inertia being roughly equal and considerably larger than the third(I_A).[16] Two of the three a.c.f. in fig. 2 decay similarly and much faster than the third $[\langle\boldsymbol{e}_3(t)\cdot\boldsymbol{e}_3(0)\rangle]$. This means that the 'tumbling' of the ethyl chloride molecule (reorientation of the $\boldsymbol{e}_3$ axis) is slower than its spinning (reorientation of either the $\boldsymbol{e}_1$ or $\boldsymbol{e}_2$ axes). The spinning motion is 'inertia dominated', *i.e.* the P_1 and P_2 a.c.f. of $\boldsymbol{e}_1$ or $\boldsymbol{e}_2$ are not exponential initially, but become so (fig. 2) after *ca.* 0.7 ps. The $P_1(\boldsymbol{e}_3)$ and $P_2(\boldsymbol{e}_3)$ functions, on the other hand, become exponential after the a.c.f. has dropped to *ca.* 80% of its initial value. The motion of $\boldsymbol{\mu}$ is a combination of tumbling and spinning in ethyl chloride (fig. 3). The spectral bandshapes of the liquid therefore also depend on a combination of these motions, as is the case for most asymmetric tops of C_{2v} symmetry or lower. The method of computer simulation can be used to clarify the details of these molecular dynamics in any convenient frame of reference. The analytical theory[11] of asymmetric-top rotational diffusion is usually based on the assumption that a principal frame may be found in the molecule defining three components of a friction matrix (or memory matrix). These

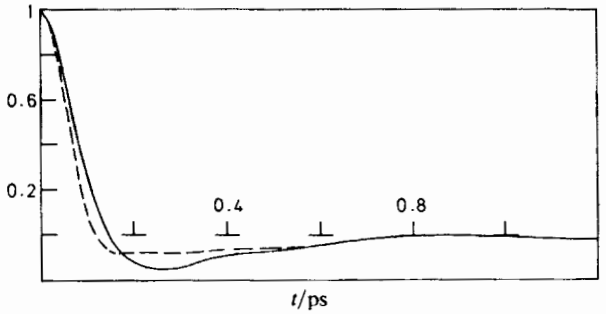

Fig. 4. Rotational velocity a.c.f. at 293 K. (———) $\langle \dot{\boldsymbol{e}}_1(t) \cdot \dot{\boldsymbol{e}}_1(0) \rangle / \langle \dot{e}_1^2 \rangle$ and (– – – –) $\langle \dot{\boldsymbol{u}}(t) \cdot \dot{\boldsymbol{u}}(0) \rangle / \langle \dot{u}^2 \rangle$.

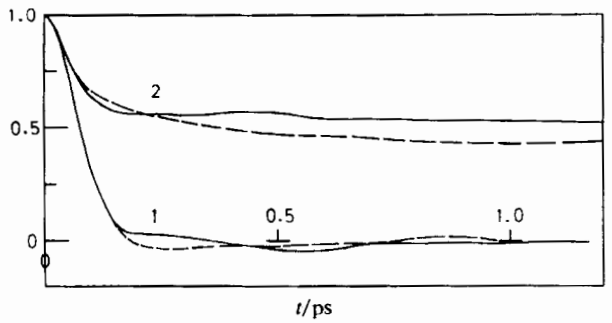

Fig. 5. (———) Angular velocity a.c.f. at 293 K: $\langle \boldsymbol{\omega}(t) \cdot \boldsymbol{\omega}(0) \rangle / \langle \omega^2 \rangle$; (1) $\langle \boldsymbol{\omega}(t) \cdot \boldsymbol{\omega}(t) \boldsymbol{\omega}(0) \cdot \boldsymbol{\omega}(0) \rangle / \langle \omega^4 \rangle$ and (2) $\langle \boldsymbol{\omega}(t) \cdot \boldsymbol{\omega}(0) \rangle / \langle \omega^2 \rangle$. (– – –) Angular momentum a.c.f.: (1) and (2) as above.

components are used in phenomenological equations such as the Euler–Langevin equations.[11] It is not always clear whether the frictional frame is the same as that of $\boldsymbol{\alpha}$ or $\boldsymbol{\mu}$ or of the moment of inertia tensor $\mathbf{I}$. This makes the theory over complicated and decreases its usefulness for low-symmetry molecules when used in the absence of numerical information from computer simulation.

The rotational velocity autocorrelation functions of $\dot{\boldsymbol{e}}_1$, $\dot{\boldsymbol{e}}_2$ and $\dot{\boldsymbol{e}}_3$ are illustrated in fig. 4, together with that of $\dot{\boldsymbol{u}}$, the derivative of the dipole unit vector. The latter effectively defines[11] the far-infrared absorption of ethyl chloride for the first time. It will be interesting to measure the true (experimental) power absorption coefficient by interferometry and compare it with the simulation.

The basically important functions in any treatment of rotational molecular diffusion in liquids are the angular velocity and angular momentum autocorrelation functions: respectively $\langle \boldsymbol{\omega}(t) \cdot \boldsymbol{\omega}(0) \rangle / \langle \omega^2 \rangle$ and $\langle \boldsymbol{J}(t) \cdot \boldsymbol{J}(0) \rangle / \langle J^2 \rangle$. In general, these do not decay in the same way with time for any symmetry lower than T_d, and this is corroborated in fig. 5 for ethyl chloride. In fig. 5 we have also plotted the second moment a.c.f., which decays to a constant level depending on the nature of the equilibrium statistics. The a.c.f. in fig. 5 attain a Gaussian level as $t \to \infty$, but are transiently non-Gaussian.

The same is true for the linear, centre-of-mass velocity a.c.f. and its second moment (fig. 6). The analytical Gaussian curve[11] is shown in this figure as a dashed

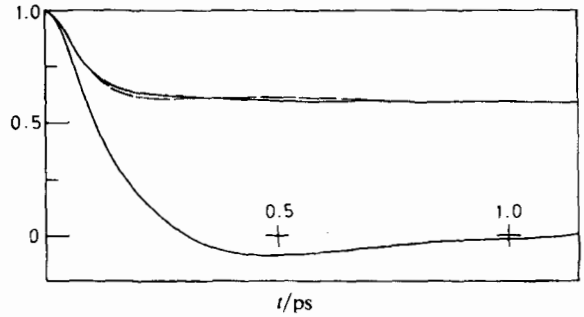

Fig. 6. Linear centre-of-mass velocity a.c.f. at 293 K. Bottom curve: $\langle \boldsymbol{v}(t) \cdot \boldsymbol{v}(0) \rangle / \langle v^2(0) \rangle$; top curves: $\langle \boldsymbol{v}(t) \cdot \boldsymbol{v}(t) \boldsymbol{v}(0) \cdot \boldsymbol{v}(0) \rangle / \langle v^4 \rangle$ and (- - -) $\frac{3}{5}[1 + \frac{2}{3}(\langle \boldsymbol{v}(t) \cdot \boldsymbol{v}(0) \rangle / \langle v^2 \rangle)^2]$, the second moment implied by Gaussian statistics.[11]

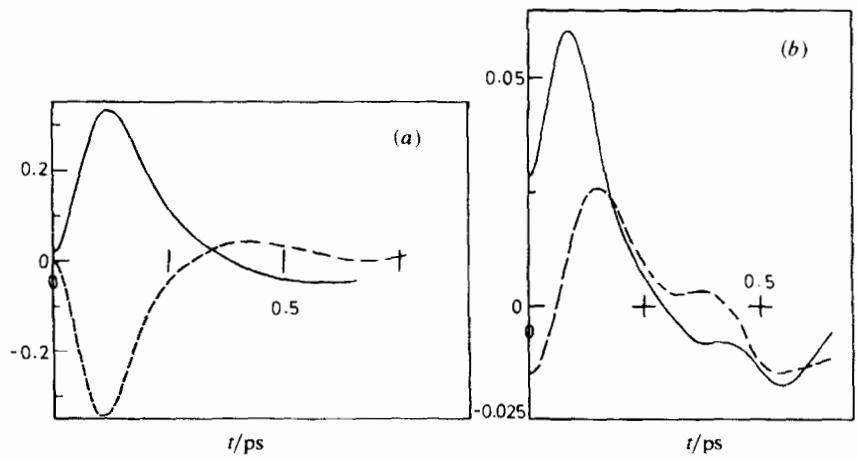

Fig. 7. (*a*) (———) (1, 2) element of the rotating frame matrix $\langle \boldsymbol{v}(t) \boldsymbol{J}^{\mathrm{T}}(0) \rangle$ at 293 K, normalised as: $\langle v_1(t) J_2(0) \rangle / (\langle v_1^2 \rangle^{1/2} \langle J_2^2 \rangle^{1/2})$; (- - -) (2, 1) element. (*b*) As for (*a*), (- - - -) (3, 2) element, (———) (2, 3) element. Note that these are very much smaller in magnitude than the (1, 2) or (2, 1) elements.

line. Both the linear and angular velocity a.c.f. have a characteristically long negative tail at intermediate times.

The Interaction of Rotation and Translation. Ciccotti *et al.*[17] have shown recently that one of the correct ways of looking at this interaction is in a rotating frame of reference. We have chosen the principal moment of inertia frame[3,4] for convenience, and constructed the autocorrelation matrix $\langle \boldsymbol{v}(t) \boldsymbol{J}^{\mathrm{T}}(0) \rangle$ in this frame. Our computations show that there are four finite elements of this matrix for $t > 0$. These are illustrated, suitably normalised, in fig. 7. The (1, 2) and (2, 1) elements are mirror images and are much greater in 'intensity' than the (3, 2) and (2, 3) elements. The other five elements are buried in the computer noise. The noise level in fig. 7 may be roughly gauged by the fact that all elements should vanish by symmetry at $t = 0$. The maximum 'intensity' of the (1, 2) and (2, 1) elements (± 0.33) is the largest we have yet observed,[3,4] implying that rotation/translation

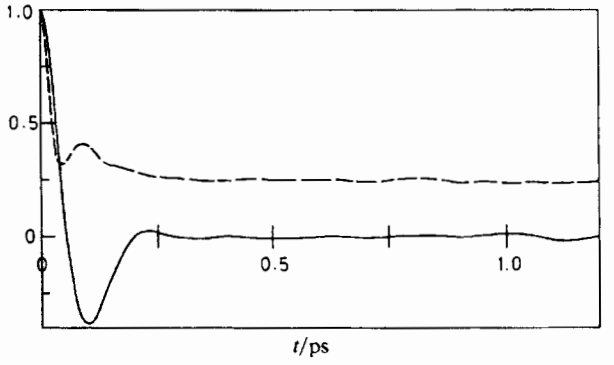

Fig. 8. (———) Torque a.c.f. at 293 K. (– – –) Second moment.

coupling in C_2H_5Cl is a significant factor in the exact treatment of its molecular dynamics in the liquid phase. This may be interpreted qualitatively by the fact that the centre of mass (fig. 1) is so close to the relatively heavy Cl atom that it is not possible for the molecule to rotate in its own volume when subjected to disturbance from the fields of its nearest neighbours. The result of fig. 7 contrasts strongly with the equivalent for chloroform,[4] where the rotation/translation coupling is vanishingly small in all elements of $\langle \boldsymbol{v}(t)\boldsymbol{J}^{\mathrm{T}}(0)\rangle$ of the rotating frame.

The third and fourth non-vanishing elements, (3, 2) and (2, 3), are far smaller in intensity but more oscillatory than the other two [fig. 7(*b*)].

There is no analytical theory available yet to describe these results, even in a qualitative manner. This is the case because the phenomenological theories[11] average out the effect of the interaction potential and effectively decouple rotation from translation. The problem facing phenomenological theoreticians is that of predicting the appearance of the non-vanishing elements of $\langle \boldsymbol{v}(t)\boldsymbol{J}^{\mathrm{T}}(0)\rangle$, their correct symmetry and intensity characteristics. The same, basic theoretical structure should also be capable of dealing with higher derivative a.c.f. such as that of the torque, illustrated in fig. 8 with its second moment. The latter attains a constant, Gaussian level of *ca.* 0.24 as $t \rightarrow \infty$, and decays initially faster than the first moment a.c.f. The most promising lines of approach seem to be the non-linear method of Grigolini and coworkers,[18–23] based on the synergetic philosophy developed by Haken and others.

SUPERCOOLED LIQUID AT 118 K AND 1 bar

Two of the most important indications produced by the computer simulation are summarised in fig. 9 and 10 for the liquid supercooled at 1 bar to 118 K. The P_1 and P_2 orientational a.c.f. of $\boldsymbol{e}_1$, $\boldsymbol{e}_2$, $\boldsymbol{e}_3$ and $\boldsymbol{\mu}$ are clearly not exponential in nature in the interval to 1.0 ps (fig. 9), and for $t > 1.0$ they tail, on this scale, parallel to the time axis. This shows clearly the validity of the (α, β, γ) hypothesis of Evans *et al.*[11] which links the far-infrared (γ) part of the loss process in a supercooled liquid to its α (and β) components, which appear as the dielectric loss curves at lower frequencies.[24] The correlation times in fig. 9 are effectively infinite (on the ps scale of the abscissa), meaning that the fast process out to 1.0 ps from $t = 0$ evolves into one taking place on an immensely slower time scale. This dynamical process contrasts greatly with that observable in our parallel simulations[3,4] of the rotator phases of t-butyl chloride and bromoform. In the rotator phase the P_1 and P_2 functions remain similar to their liquid-phase counterparts.

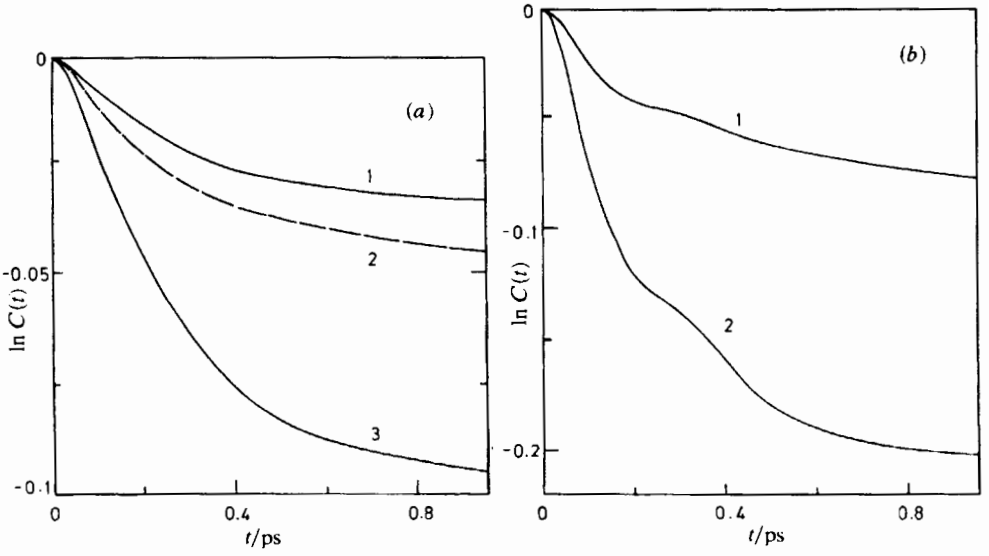

Fig. 9. Orientational a.c.f. for supercooled ethyl chloride at 118 K, plotted as ln (correlation function) against time. (*a*) (1) $P_1(e_3)$, (2) $P_1(u)$ and (3) $P_2(e_3)$. Note that the slope at long times is almost parallel to the time axis (>1.0 ps). (*b*) (1) $P_1(e_2) = P_1(e_1)$ (on this scale) and (2) $P_2(e_2) = P_2(e_1)$.

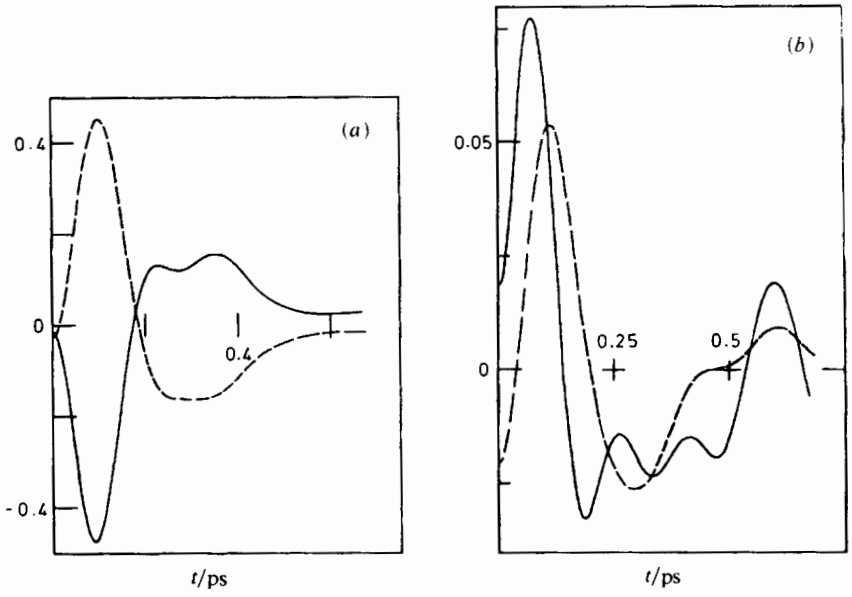

Fig. 10. Elements of the rotating frame matrix $\langle v(t)J^{T}(0)\rangle$ at 118 K, supercooled liquid, showing very strong rotation/translation coupling. (*a*) (- - - -) (1, 2) element and (———) (2, 1) element. (*b*) (- - - -) (3, 2) element and (———) (2, 3) element.

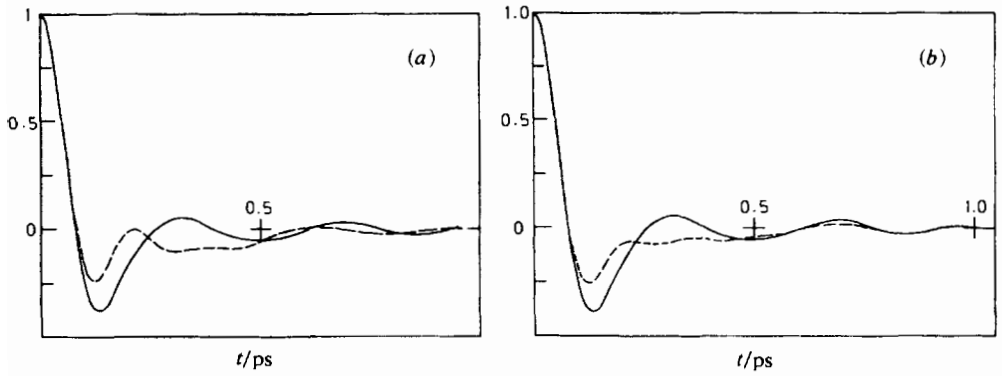

Fig. 11. Rotational velocity a.c.f. at 118 K. (*a*) (– – – –) $\langle \dot{e}_3(t) \cdot \dot{e}_3(0) \rangle / \langle \dot{e}_3^2 \rangle$ and (———) $\langle \dot{e}_2(t) \cdot \dot{e}_2(0) \rangle / \langle \dot{e}_2^2 \rangle$. (*b*) (– – – –) $\langle \dot{\boldsymbol{u}}(t) \cdot \dot{\boldsymbol{u}}(0) \rangle / \langle \dot{u}^2 \rangle$ and (———) $\langle \dot{e}_1(t) \cdot \dot{e}_1(0) \rangle / \langle \dot{e}_1^2 \rangle$. Compared with the curves of fig. 4 these are more oscillatory and cut the time axis earlier. The Fourier transform of $\langle \dot{\boldsymbol{u}}(t) \cdot \dot{\boldsymbol{u}}(0) \rangle / \langle \dot{u}^2 \rangle$ gives the Reid–Evans γ process[24] of the far-infrared.[11]

Fig. 10 illustrates the non-vanishing (1, 2), (2, 1), (2, 3) and (3, 2) elements of the rotating-frame matrix of a.c.f.: $\langle \boldsymbol{v}(t) \boldsymbol{J}^{\mathrm{T}}(0) \rangle$, suitably normalised at the time origin. The maximum (or minimum) values of the symmetric (1, 2) and (2, 1) elements are the biggest we have yet observed in our simulation programme.[3,4] This means that the mutual influence of rotation and translation is fundamentally important in influencing the nature of the supercooled liquid state of C_2H_5Cl and, by implication, the supercooled liquid state in general. We need hardly point out that there exists no analytical method able to explain these correlation functions from a simple hypothetical base. Their existence and magnitude is clear beyond doubt, however, and they would probably be effective in setting up long-lived vortices in the supercooled liquid if the rotation/translation become coherent on a macroscopic scale. The curves of fig. 4 are examples of how a computer simulation may be used to provide otherwise unobtainable information on a fundamental level.

In fig. 11 we illustrate the four rotational velocity a.c.f.: (*a*) $\langle \dot{e}_1(t) \cdot \dot{e}_1(0) \rangle / \langle \dot{e}_1^2 \rangle$, (*b*) $\langle \dot{e}_2(t) \cdot \dot{e}_2(0) \rangle / \langle \dot{e}_2^2 \rangle$, (*c*) $\langle \dot{e}_3(t) \cdot \dot{e}_3(0) \rangle / \langle \dot{e}_3^2 \rangle$ and (*d*) $\langle \dot{\boldsymbol{u}}(t) \cdot \dot{\boldsymbol{u}}(0) \rangle / \langle \dot{u}^2 \rangle$, where $\boldsymbol{u}$ is the dipole unit vector. The fourth function is observable as a far-infrared spectrum by Fourier transformation[11] and is more oscillatory than its equivalent (fig. 4) at 293 K. It cuts the time axis earlier, which means that the far-infrared spectrum (termed the γ process by Evans *et al.*[11]) is shifted to higher frequencies in the supercooled liquid and considerably sharpened. This is precisely what is observed experimentally[11] for a variety of dipolar solutes in supercooled decalin.[24] Fig. 9 and 11 together corroborate the (α, β, γ) hypothesis of Reid and Evans,[24] *i.e.* the far-infrared process (fig. 11) is the high-frequency (γ) adjunct of a multi-decade relaxation absorption representing the evolution of the molecular dynamics from picosecond time-scales (fig. 11) to immensely longer ones, illustrated by the effectively 'infinite' correlation times of fig. 9. This again illustrates the predictive power of the computer simulation method, starting from a simple model of the pair potential.

The molecular angular-velocity (fig. 12) and angular-momentum (fig. 13) a.c.f. in supercooled ethyl chloride are oscillatory. The second moment a.c.f. $\langle \boldsymbol{\omega}(t) \cdot \boldsymbol{\omega}(t) \boldsymbol{\omega}(0) \cdot \boldsymbol{\omega}(0) \rangle / \langle \omega^4 \rangle$ and $\langle \boldsymbol{J}(t) \cdot \boldsymbol{J}(t) \boldsymbol{J}(0) \cdot \boldsymbol{J}(0) \rangle / \langle J^4 \rangle$, respectively, show that the governing statistics are transiently non-Gaussian, but both functions become

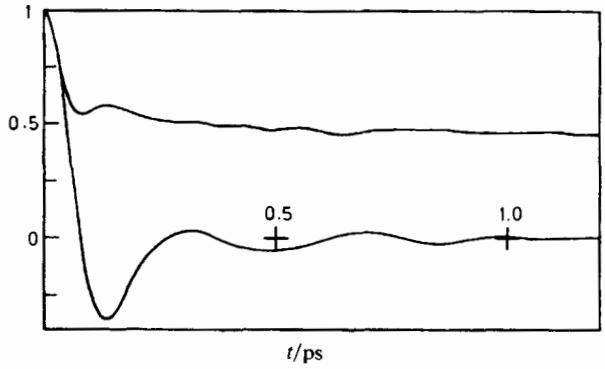

Fig. 12. Angular velocity a.c.f. at 118 K. Lower curve: $\langle \boldsymbol{\omega}(t) \cdot \boldsymbol{\omega}(0) \rangle / \langle \omega^2 \rangle$; upper curve: $\langle \boldsymbol{\omega}(t) \cdot \boldsymbol{\omega}(t)\boldsymbol{\omega}(0) \cdot \boldsymbol{\omega}(0) \rangle / \langle \omega^4 \rangle$.

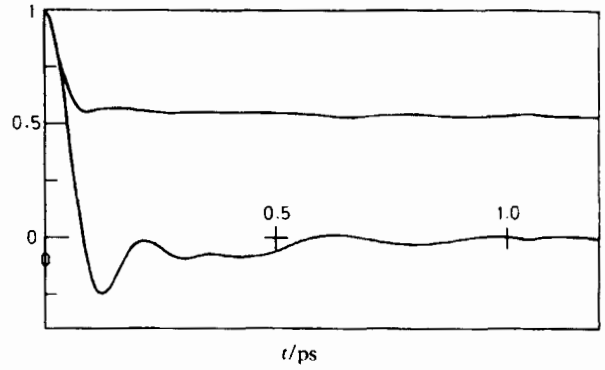

Fig. 13. As for fig. 12 for angular momentum ($\boldsymbol{J}$).

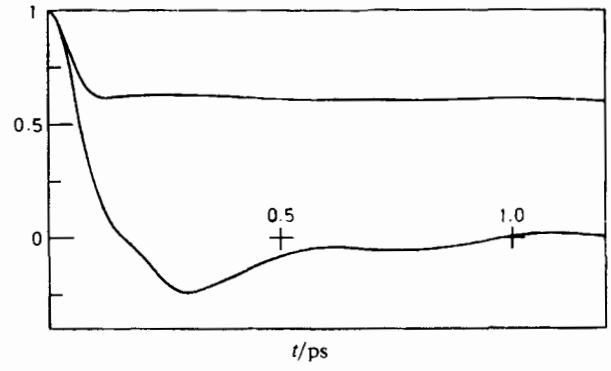

Fig. 14. As for fig. 12 for centre-of-mass linear velocity (v).

Gaussian at equilibrium. It is clear in consequence that a non-linear general theory of the liquid state is needed to account for these results. The work of Grigolini and coworkers[18-23] is a good basis for their description.

The linear, centre-of-mass velocity autocorrelation function (fig. 14) is a compound of two types of oscillation. It seems clear from fig. 10 that the origin of the

faster oscillations seen superimposed on the main functional form in fig. 14 is rotation/translation coupling. The a.c.f. of fig. 14 is computed in the laboratory frame of reference, while the rotation/translation effects of fig. 10 are directly observable only in a rotating frame. It is important to realise, however, that rotation/translation coupling indirectly affects all the laboratory frame a.c.f. of supercooled liquid ethyl chloride. This is simply due to the fact that the molecule cannot rotate without displacing simultaneously its centre of mass. Fig. 14, in conclusion, therefore, illustrates the effect of very strong rotation/translation coupling on the centre-of-mass velocity a.c.f. in the laboratory frame of reference.

CONCLUSIONS

The computer simulation method has been used to investigate in detail the molecular dynamics of the C_1 symmetry molecule C_2H_5Cl.

An original feature of the investigation is the discovery of strong rotation/translation coupling, using a rotating frame of reference.

The molecular dynamical characteristics are strikingly different at 293 K (the liquid under its own vapour pressure) and at 118 K (supercooled). In the supercooled condition the orientational a.c.f. of the dipole unit vector, $\boldsymbol{u}$, decays almost infinitely slowly implying the existence of a hitherto unmeasured dielectric loss at very low frequencies. The (α, β, γ) hypothesis of Evans *et al.*[11] is corroborated by our computer simulation of the γ process[24] in the far-infrared.

We thank the S.E.R.C. for financial support and CCP5 for a listing of the original algorithm TETRAH. Dr. M. Ferrario is thanked for many useful discussions.

[1] C. R. Miller and S. L. Gordon, *J. Chem. Phys.*, 1970, **53**, 3531.
[2] B. Lassier and C. Brot, *J. Chim. Phys.*, 1968, **65**, 1723.
[3] M. W. Evans and G. J. Evans, *J. Chem. Soc., Faraday Trans 2*, 1983, **79**, 153.
[4] M. W. Evans, M. Ferrario, G. J. Evans and V. K. Agarwal, *J. Chem. Soc., Faraday Trans 2*, 1983, **79**, 137.
[5] C. Tsonopoulos, *AIChE J.*, 1975, **21**, 827.
[6] K. Bohmhammel and W. Mannchen, *Z. Phys. Chem.*, 1971, **248**, 230.
[7] W. S. Haworth and L. E. Sutton, *Trans. Faraday Soc.*, 1971, **67**, 2907.
[8] G. Martin, *J. Chim. Phys.*, 1967, **64**, 347.
[9] A. N. M. Barnes, D. J. Turner and L. E. Sutton, *Trans. Faraday Soc.*, 1971, **67**, 2902.
[10] T. McMullen, E. D. Crozier and R. McIntosh, *Can. J. Chem.*, 1968, **46**, 2945.
[11] M. W. Evans, G. J. Evans, W. T. Coffey and P. Grigolini, *Molecular Dynamics* (Wiley Interscience, New York, 1982), chap. 7.
[12] K. A. Strong, R. M. Brugger and R. J. Pugmire, *J. Chem. Phys.*, 1970, **52**, 2277.
[13] J. R. Durig, C. M. Player and J. Bragin, *J. Chem. Phys.*, 1971, **54**, 460.
[14] J. E. Mark and C. Sutton, *J. Am. Chem. Soc.*, 1972, **94**, 1083.
[15] G. Del Re, *J. Chem. Soc.*, 1958, 4031.
[16] R. S. Wagner and B. P. Dailey, *J. Chem. Phys.*, 1954, **22**, 1459.
[17] G. Ciccotti, A. Bellemans, and J-P. Ryckaert, *Mol. Phys.*, 1981, **44**, 979.
[18] P. Grigolini, *Mol. Phys.*, 1976, **31**, 1717.
[19] P. Grigolini, *Nuovo Cimento B*, 1981, **63**, 174.
[20] P. Grigolini, *J. Chem. Phys.*, 1981, **74**, 1517.
[21] P. Grigolini, *Chem. Phys.*, 1979, **38**, 389.
[22] M. W. Evans, P. Grigolini and F. Marchesoni, *Chem. Phys. Lett.*, submitted for publication.
[23] M. W. Evans, P. Grigolini and F. Marchesoni, in preparation.
[24] C. J. Reid and M. W. Evans, *J. Chem. Phys.*, 1982, **76**, 2576.

(PAPER 2/1738)